Pertanika J. Sci. & Technol. 23 (1): 153 - 161 (2015)

SCIENCE & TECHNOLOGY

Journal homepage: http://www.pertanika.upm.edu.my/

Microstructure Analysis, Physical and Thermal Properties of Al_2O_3-Al_2TiO_5 Functionally Graded Ceramics for the Application of Car Brake Rot

Rong Kimberly, F. P.[2], Oo, Z.[1*] and Sujan, D.[2]

[1]*Department of Electrical and Computer Engineering, School of Engineering and Science, Curtin University, Sarawak Malaysia, CDT 250, Senadin, Miri, Malaysia*

[2]*Department of Mechanical Engineering, School of Engineering and Science, Curtin University, Sarawak Malaysia, CDT 250, Senadin, Miri, Malaysia*

ABSTRACT

Aluminium titanate (AT) (Al_2TiO_5) is a promising engineering material because of its low thermal expansion coefficient, excellent thermal shock resistance, good refractoriness and non-wetting with most metals. Functionally graded material (FGM) is generally a particulate composite with continuously varying volume fractions. FGMs are alternative materials for dental implants, building materials and ballistic protection. It has been of great interest to future engines, internal combustion engines, metal cutting and other high temperature engineering application. There has been a demand for an adequate disc brake that requires less maintenance in the automotive manufacturing industry. FGM, the next evolution of layered structure, consists of graded compositions that are dispersed across the ceramic which produces a gradual improvement in the properties across the ceramic at a steady pace.

Keywords: Functional Graded Materials, Aluminium titanate, refractory, excellent thermal shock resistance

INTRODUCTION

AT, with the pseudo-brookite structure, is the only compound in the alumina-titania system. It is an excellent refractory and thermal shock resistant material due to its relatively low thermal expansion coefficient (1 x 10^{-6} $^{o}C^{-1}$), thermal conductivity (0.9 to 1.5 W/m.K) and high melting point (1860ºC) (Kato *et al.*, 1980). Due to the effects of atmosphere and annealing time on the thermal stability of Al_2TiO_5- based, Al_2TiO_5 is stable with no apparent phase decomposition for up to 5h at 1100ºC in air and becomes unstable between 1100-1280ºC when it undergoes a eutectoid-

Article history:
Received: 7 November 2013
Accepted: 18 January 2014

E-mail addresses:
zeya.oo@curtin.edu.my (Oo, Z.)
d.sujan@curtin.edu.my (Sujan, D.)
kimbuali@gmail.com(Rong Kimberly, F. P)
*Corresponding Author

ISSN: 0128-7680

like decomposition to α-Al_2O_3 and TiO_2 (rutile) (Oo, 2012). The process of decomposition in Al_2TiO_5 is reversible at above 1350ºC (Oo, 2012). Currently, the braking system is the most important thing for the transportation affairs in the world. The traditional disc brake rotors in use today are fabricated by gray cast iron (Borgiolo *et al*., 2004). Jun Qu and co-workers (2009) presented the feasibility of using excellent coefficient friction level (0.35-0.50) by using oxygen-diffused titanium a candidate brake rotor material. High density, thermal conductivity and specific heat capacity of gray cast iron are 7.6 g/cm^3, 47.3 W/mºC and 0.498 J/g. K, respectively (Kimberly *et al*., 2011). Till now, the best candidate brake rotor material for the future generation replacement of the car brake rotors in terms of the relationship between high speed and less coefficient of friction is still unsatisfactory yet. Therefore, it is anticipated that Al_2TiO_5 FGM ceramics may replace conventional gray cast iron for better thermal performance in car brake rotor. Moreover, due to its low density compared to gray cast iron, Al_2TiO_5 FGM ceramics, it is a fuel saving option for car brake rotor (Sujan *et al*., 2012). At present, there has been no significant research performed on the application of FGM in the car brake rotor manufacturing. In this paper, an assessment of the microstructure analysis and a preliminary investigation of the physical and thermal properties of FGM Al_2O_3- Al_2TiO_5 (AT) are presented.

MATERIALS AND METHODS

Sample Preparation

Al_2TiO_5 (AT) Aluminium titanate was synthesized by molar ratio method, using one mole of Al_2O_3 and one mole of TiO_2. Two different FGM samples group preparations were introduced. The first sample group preparation, based on the creation of thin interface of graded (A, B, and C) three batches of Al_2O_3/Al_2TiO_5 composite without layers, was sandwiched between an outer layer of 100%Al_2O_3 and 100%AT with the thickness range from 0.3cm, 0.4 cm and 0.5 cm, respectively. The second sample group preparation provided the FGM samples with the sandwich, graded (D, E, F, and G) four batches layers of 50%Al/50%AT, 75%Al 25%AT, 25% AT and 25%Al/75% AT, with the thickness range from 0.3cm to 0.5 cm, respectively. The samples were uniaxial die-pressed at 5000 PSI for 20 seconds by a Blackhawk Uniaxial Press to allow solidification. The FGM samples were sintered at 1200°C for an hour by using LENTON AWF 12/12.

Radial Shrinkage

Radial shrinkages were measured for all the seven batches of the FGM samples using Vernier Caliper. The diameters of the FGM samples were measured from the top surface (Al_2O_3 layer) with percentage increments until the bottom surface (Al_2TiO_5 layer). The radial shrinkage (Sr) was calculated using equation (1).

$$S_r = \frac{D - D_{measured}}{D} \times 100 \qquad (1)$$

D = diameter (cm),

$D_{measured}$ = measured diameter (cm)

Density and Porosity

The FGM samples 100%Al_2O_3/100%Al_2TiO_5, with the thickness of 0.4 cm and 0.5 cm, 50%Al_2O_3/50% Al_2TiO_5 sandwich layers thickness of 0.3 cm and 0.4 cm were utilized and measured for the density and porosity test. Firstly, the dry, sintered and cooled samples were weighed using a digital weighing scale with an uncertainty of ± 0.01g. Secondly, the samples were soaked in water for approximately 24 hours before being they were weighed again, suspended in air as well as suspended in de-ionized water. Finally, bulk density (D_b), apparent solid density (D_{as}) and apparent porosity (P_a) were then calculated using the formulas:

$$D_b = \frac{m_D}{m_s - m_i} \times D_i$$

$$D_{as} = \frac{m_D}{m_D - m_i} \times D_i \qquad (2)$$

$$P_a = \frac{m_s - m_D}{m_s - m_i} \times 100$$

m_D = Mass of dry sample (g)
m_i = Mass of sample saturated with and suspended in water (g)
m_s = Mass of sample saturated with water and suspended in air (g)
D_i = Density of water (1 g m^{-3})

Thermal Conductivity

The FGM samples 50%Al_2O_3/50%Al_2TiO_5 (thickness=0.5 cm) and 75%Al_2O_3 + 25% Al_2TiO_5 (thickness=0.3cm) /25%Al_2O_3 + 75%Al_2TiO_5 (thickness=0.3 cm) were used to test for the thermal conductivity by using the Graded Heat Flow method.

Scanning Electron Microscopy

Scanning Electron Microscopy (SEM) has been used for analyzing the surface imaging of samples, mostly showing the cross-sectional microstructure of the materials. Due to the type of signals produced by backscattered electrons (BSE), the decomposition characteristics of Al_2TiO_5 at 1100°C for coarse grain, medium grain and fine grain are shown in Figures 4 (a-c).

RESULTS AND DISCUSSION

Radial Shrinkage

Radial shrinkage (%) with percentage distance for all FGM seven groups are shown in Figures 1-3. It is very evident that the FGM samples have undergone non-uniform shrinkage. One of the factors that leads to the non-uniformly shrinkage is the porosity of both Al_2O_3 and Al_2TiO_5.

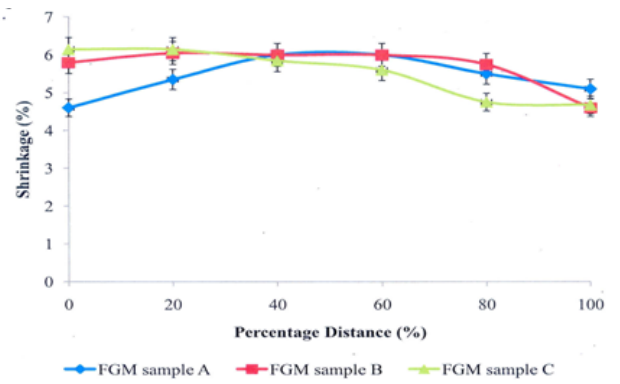

Fig.1. Shrinkage (%) vs. percentage distance for A, B, and C, FGM layers

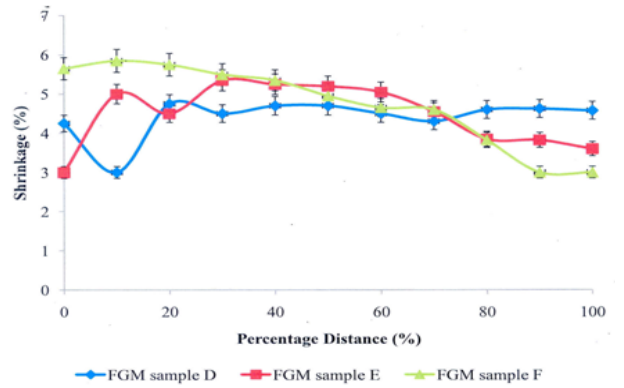

Fig.2. Shrinkage (%) vs. percentage distance for D, E and F, FGM layers

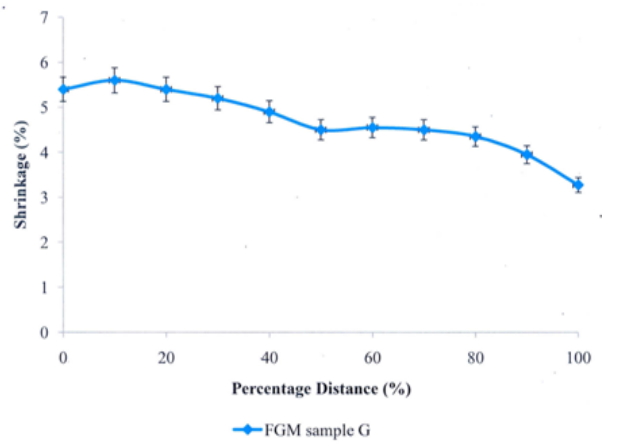

Fig 3. Shrinkage (%) vs. percentage distance for FGM – G

Shrinkage plays an important role in the suppression of defect forming during sintering. When a ceramic is sintered, it shrinks and experiences a reduction of porosity and an improvement in mechanical integrity. These changes occur due to the coalescence of the powder particles into a dense mass, where the reduction in total particle surface area is caused by surface energies being larger in magnitude than grain boundary energies. Necks are formed along the contact regions between adjacent particles during the initial sintering stage. Grain boundary then forms within each neck and every interstice between the particles becomes a pore (Callister, 2003). Shrinkage was measured for all the samples in the first group A, B, and C (sintered at 1200˚C for 1 hour) and second group, D, E, and F (sintered at 1200˚C for 1 hour), averaged and then grouped into three groups, depending on the thickness of the outermost alumina layer and the temperature they were sintered at 1200°C. The results were then graphed using the surface of the alumina layer as the starting point (Figures 1-3).

The effect is due to the fact that the two materials of alumina and aluminium titanate have vastly differing coefficients of thermal expansion and porosity. Thus, their shrinkage rates would be vastly different. The aluminium titanate is vastly more porous than the alumina, and thus does not incur shrinkage at the rate that the alumina would because it possesses greater pore size that will take longer to reduce in size. The large difference in thermal expansion coefficients also depicts the difference in dimensional change with temperature variations, in such that alumina dimensions will change at a rate of approximately eight times more than that of aluminium titanate. The effects of non-uniform shrinkage could be lessened by introducing more discrete steps across the cross-section of the sample of the sample.

Density and Porosity

The FGM samples B, C, D and F were tested for their density and porosity. The calculated bulk density and apparent porosity are tabulated in Table 1.

TABLE 1: Bulk Density and porosity values for the FGM samples (Tatt, 2010)

FGM sample	Bulk Density (ρ_s g/cm^3)	Apparent Porosity (%)
B	15.7	21.9
C	15.1	23.4
D	9.76	38.4
E	10.1	38.6

The results that can be observed are the bulk density decreases while the apparent porosity increases with the introduction of the intermediate functionally graded layer (50% Al_2O_3 + 50% Al_2TiO_5). This may be the influence of Al_2TiO_5 on the FGM samples as a whole as Al_2TiO_5 is less dense than Al_2O_3. Al_2TiO_5 has a very low coefficient of thermal expansion and a low bulk density compared to Al_2O_3 and thus a build-up of residual stress will occur during sintering, which tends to hinder densification due to debonding between the grains of Al_2O_3 and Al_2TiO_5.

Another factor is that Al_2TiO_5 has large pores; therefore, there are many larger interstices between the particles which create larger pores that need to be reduced. This results in the lowering of the overall density of the material. Still, the Al_2O_3 layer and the Al_2TiO_5 layer would not see much of a reduction in density compared to their stand alone counterparts.

Thermal Conductivity

From the second group of FGM, the F and G samples were tested for the thermal conductivity by using the graded heat flow method (see Fig.4), in which the temperatures from both Al_2O_3 (alumina) side (heat source) and the Al_2TiO_5 (AT) side was measured. The results are shown in Table 2.

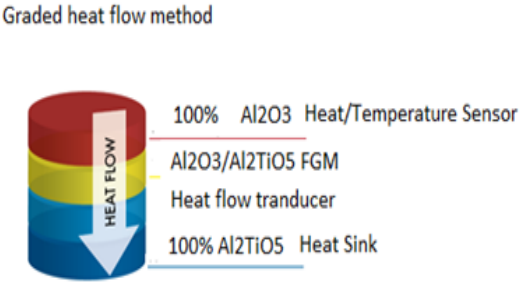

Fig. 4. Thermal conductivity tested by using the Graded heat flow method (Adopted from http//www. Thermalphysics.com)

Table 2: Bulk Density and porosity values for the FGM samples

FGM samples	Thermal conductivity, k (W/m. K)
F	267.29 ± 0.02
G	256.33 ±0.02

The resulting thermal conductivity is significantly higher compared to stand alone alumina and Al_2TiO_5 (AT). It is clear that the influence of alumina on the FGM samples as a whole is greater than Al_2TiO_5 (AT). In addition, Al_2TiO_5 (AT) also increased due to the FGM arrangement.

Scaning Electron Microscopy Analysis

The microstructure of as-sintered Al_2TiO_5 sample is shown in Fig.4 (a, b and c) where relatively large and smooth grains of 10-20 μm formed with occasional appearance. When this sample was isothermally decomposed at 1100°C for 22 h, finer grains of rutile (white) and α-Al_2O_3 (dark) can be seen to form in-situ within the original Al_2TiO_5 (light gray) grain as shown in Figures 4 (a) and (b). The microstructure of the as-sintered Al_2TiO_5 sample is shown in Fig. 4 (a, b and c), where relatively large and smooth grains of 10-20 μm formed with occasional appearance.

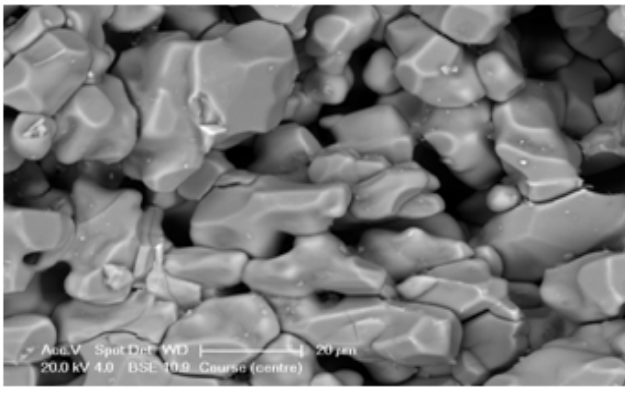

(a)

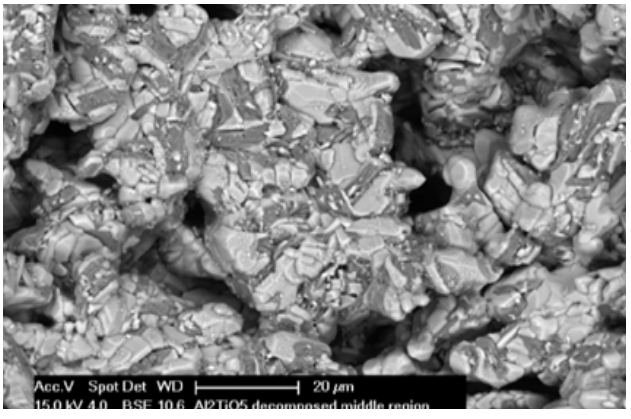

(b)

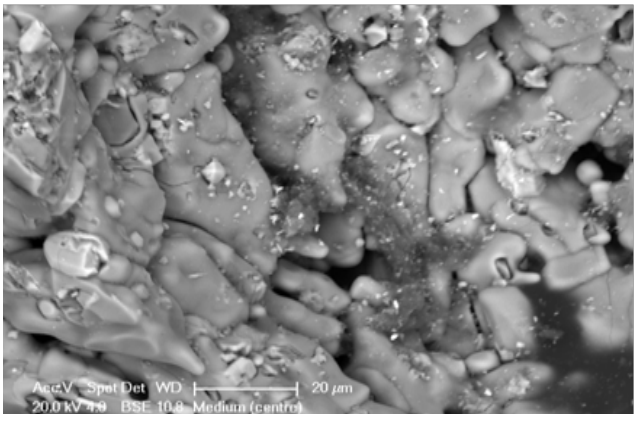

(c)

Fig. 4 (a-c). Back-scattered electron micrographs showing the microstructure of (a) as sintered Al_2TiO_5 coarse grain size and (b) isothermally decomposed Al_2TiO_5 fine grain size at 1100ºC for 22 h. (c) Al_2TiO_5 medium grain size decomposed at 1100 ºC for 22 h Legend: White phase is rutile (TiO_2), light gray is Al_2TiO_5, dark gray is α- Al_2O_3 and black are pores and cracks (Adopted from Oo, 2012).

When this sample was isothermally decomposed at 1100°C for 22 h, finer grains of rutile (white) and α-Al_2O_3 (dark) can be seen to form in-situ within the original Al_2TiO_5 (light gray) grain as shown in Fig. 4(a) and 4(b) (Oo, 2012). This physical separation or decomposition of Al_2TiO_5 into finer grains of alumina and rutile has not resulted in observable shrinkage or disintegration of the decomposed sample. In fact, the decomposed sample appears to be harder and stronger due to the presence of alumina and rutile in the microstructure. However, the development of secondary intragranular porosity can be seen in the decomposed microstructure which concurs with the work of Hennicke and Lingenberg (Manurung, 2001).

CONCLUSION

On the basis of the above finding, the following are the physical and thermal properties of Al_2O_3-Al_2TiO_5 main points that can be summarized. The radial shrinkages of FGM Al_2O_3-Al_2TiO_5 were observed by using the defects concepts due to the sintering process. Meanwhile, the density, porosity and thermal conductivity of FGM Al_2O_3-Al_2TiO_5 were studied and the influence of Al_2TiO_5 is the most significant for decomposition at 1100°C. Hence, the microstructure evaluation for the combination of 50% Al_2O_3 and 50% Al_2TiO_5, 75% Al_2O_3 and 25% Al_2TiO_5, 25% Al_2O_3 and 75%Al_2TiO_5 were observed and verified the results of physical properties.

Isothermally decomposition of Al_2TiO_5 was confirmed by Scanning-Electron Microscope. The typical microstructure of as-sintered coarse-grained Al_2TiO_5 prior to thermal ageing can be attributed to the pronounced thermal expansion anisotropy of Al_2TiO_5 during cooling from an elevated temperature. The presence of these microcracks is believed to impart a low fracture strength but high thermal shock resistance to Al_2TiO_5 (Oo, 2012). Following isothermal-ageing in air at 1000˚C for 14 h, both needle-like and angular particles could be seen to form on the surface of Al_2TiO_5 grains. Those nano-sized particles were identified alpha-Al_2O_3 and TiO_2 at the edge and centre of the coarse, medium and fine grained samples of isothermally decomposed Al_2TiO_5 during 10 h (Oo, 2012). It should be noted that the decomposition characteristics of Al_2TiO_5-based ceramics at 1100˚C is highly significant. On the other hand, an appropriate coefficient of friction level, wear volume and wear rate of Al_2O_3-Al_2TiO_5 FGM car brake rotor still need to be studied for the commercial brake system.

ACKNOWLEDGEMENTS

This project was funded by the Curtin Sarawak Collaboration Research (CSCR), Approval number 4011, 2010-2012. The authors would like to thank to Mr Jonathan Yong Chung Tatt, Tokuyama (Malaysia) Sdn Bhd., B.E. (Mechanical Engineer 2010), for his contribution in conducting experimentation on the density, porosity and thermal conductivity of FGM.

REFERENCES

Borgioli, E., Galvanetto, E., Fossati, A., & Pradelli, G. (2004). Glow-Discharge and Furnace Treatments of Ti-6Al-4V, *Surface Coating Technology, 184*, 255-262.

Callister, W. D. (2003). *Materials Science and Engineering, An Introduction* (6th edition). New York: John Wiley & Sons, Inc.

Kato, E., Daimon, K., & Takahashi, K. 1980. Decomposition Temperature of beta-Al_2TiO_5. *Journal of the American Ceramic Society, 63*, 355-356.

Kimberly, F. P. R., Gorin, A., Sujan, D., & Oo, Z. (2012). On the Problem of Novel Composite Materials Development for Car Brake Rotor. *International Journal of Engineering and Physical Sciences, 6*, 333-336.

Manurung, P. (2001). *Microstructural Design and Characterisation of Alumina/Aluminium Titanate Composites*. (PhD Thesis). Curtin University, Australia.

Oo, Z. (2012). *Charactgerisation of Thermal Stability, Microstructures and Properties of Al_2TiO_5- and Ti3SiC2-based Ceramics*. (Ph D Thesis). Curtin University. Australia.

Qu, J., Blau, P. J., & Jolly, B. C. (2009). Oxygen-Diffused Titanium as a Candidate Brake Rotor Material, *Wear, 267*, 818-822.

Sujan, D., Oo, Z., Hahman, M. E., Maleque, M. A., & Tan, C. K. (2012). Physio-mechanical Properties of Aluminium Metal Matrix Composites Reinforced with Alumina and Silicon Carbide. *International Journal of Engineering and Applied Sciences, 6*, 288-291.

Tatt, Y. C. (2010). Fabrication and Mechanical Properties of Functionally Graded Ceramics Al_2O_3-Al_2TiO_5. *Final Year Project Report*, Curtin University Sarawak Malaysia.